Colloids and Surfaces A: Physicochem. Eng. Aspects 382 (2011) 251–260

Contents lists available at ScienceDirect

Colloids and Surfaces A: Physicochemical and Engineering Aspects

journal homepage: www.elsevier.com/locate/colsurfa

"Reprint of Numerical simulation of multi-component mass transfer in rigid or circulating drops: Multi-component effects even in the presence of weak coupling"☆

S. Ubal[a], P. Grassia[b,*], C.H. Harrison[b], W.J. Korchinsky[b]

[a] Instituto para el Desarrollo Tecnológico de la Industria Quimica (INTEC), Güemes 3450, 3000 Santa Fé, Argentina
[b] CEAS, The Mill, University of Manchester, Oxford Rd, Manchester M13 9PL, UK

ARTICLE INFO

Article history:
Received 24 September 2010
Received in revised form
23 November 2010
Accepted 24 November 2010
Available online 5 May 2011

Keywords:
Multi-component mass transfer
Circulating drop model
Convective transport
Cross-stream diffusion
Mathematical modelling
Numerical analysis
Simulation
Liquid–liquid extraction

ABSTRACT

Numerical simulation results of mass transfer to and from drops with applications to liquid–liquid extraction processes are considered. Multiple solute components (specifically 2 solute components) are assumed to be present in the drop. The system is described using the theory of multi-component mass transfer, in which a flux of one component can be coupled to a concentration gradient in the other. The nominal strength of this coupling is determined by the off-diagonal elements of a diffusivity matrix. Naively it might be thought that, if the off-diagonal matrix elements are small compared to the diagonal ones, then the influence of coupling between components is essentially negligible. It is shown however that this is not always the case. Particular focus is given to the case where one solute component has an imposed concentration difference between the drop interior and the drop surface, whilst the other solute has no such difference imposed. Mass transfer is still observed for the latter component, which is a clear indication of coupling due to multi-component diffusion effects. The mass fraction of the component with no imposed concentration difference evolves first by deviating from its initial value, but later returns back to this initial value. It is possible to place a bound on the extent of this deviation in terms of the elements of the diffusivity matrix and any concentration difference imposed on the other component. Circulation flow, if present within the drop, is found only to have a weak influence on the maximum extent of the aforementioned deviation. It has however a role in speeding up the rates of deviation and subsequent return of component mass fraction compared to a non-circulating rigid drop case. Circulation also determines the order in which individual pointwise locations in the drop experience this deviation and subsequent return: only points near the drop surface experience a rapid evolution in the absence of circulation, whereas points either near the surface or near the axis evolve rapidly in the presence of circulation.

1. Introduction

Mass transfer by liquid–liquid extraction is important in many chemical engineering operations [1–5]. During liquid–liquid extraction, one or more solutes transfers to or from dispersed drops of one solvent phase to a surrounding continuous phase of an immiscible solvent. The mass transfer process is driven by diffusion from one phase to the other immiscible phase. One complicating feature however is that when more than one solute is present, it is possible to have multi-component mass transfer in which a concentration gradient of one component drives a flux of another [6–17]. In order to analyse this complicating feature it is sufficient to consider a ternary system, with two solutes and one solvent present (and this is what will be studied here), although it should be emphasised that the multi-component mass transfer theory applies more generally to a system with an arbitrary number of components.

Coupling between concentration gradients and fluxes of different components can have serious consequences for the liquid–liquid extraction process. The nominal strength of the coupling is measured by off-diagonal elements of a diffusivity matrix [16]. When these off-diagonal elements are large, strong coupling between solute components is expected, and multi-component effects certainly cannot be ignored. The converse however is not true. Even in the case where off-diagonal elements are small (compared to diagonal ones), it might not be possible to neglect

☆ The article is reprinted here for the reader's convenience and for the continuity of the special issue. For citation purposes, please use the original publication details: [Colloids Surf. A: Physicochem. Eng. Aspects 380 (2011) 6–15] doi:10.1016/j.colsurfa.2010.11.058.

* Corresponding author. Tel.: +44 0161 306 8851; fax: +44 0161 306 9321.
E-mail addresses: subal@santafe-conicet.gov.ar (S. Ubal), paul.grassia@manchester.ac.uk (P. Grassia), Carlos.Harrison@k-wac.com (C.H. Harrison), walter.korchinsky@manchester.ac.uk (W.J. Korchinsky).

0927-7757/$ – see front matter © 2010 Elsevier B.V. All rights reserved.
doi:10.1016/j.colsurfa.2011.04.021

multi-component effects altogether. Suppose, for example in the case where two solutes are present, that solute 1 is the one we are trying to transfer and solute 2 is a contaminant present in both dispersed drop and surrounding immiscible continuous phases. If the transfer of solute 1 also drives transfer of solute 2, then the concentration of solute 2 in either solvent phase will change over time, even if the concentration (or more generally chemical potential [16,18]) of solute 2 is initially equal in both phases, meaning that there is no mass transfer driving force for solute 2 on its own. It is possible that the level of the contaminant solute 2 might be acceptable initially (for some desired target product purity) but evolves over time to become unacceptable. Even very small changes in the level of solute 2 might need to be determined via the theory of multi-component mass transfer if the initial concentration level is near to some critical purity. It therefore needs to be determined under what circumstances these multi-component effects are important, and under what circumstances a simpler single component theory might be acceptable. This may depend not only on the size of the off-diagonal diffusivity matrix elements, but also on the initial and boundary conditions applied to the solute concentrations: such a case will be studied here.

Apart from multi-component effects, another complicating feature of mass transfer in liquid–liquid extraction is circulation [19–27]. It has been described [24–26] how circulation drives material around an internal stagnation point located typically quite close to the equatorial plane and at a radial coordinate about 0.7 of the radius of the drop. Circulation speeds up mass transfer compared to a rigid (non-circulating) drop by advecting material from the drop surface to the drop interior. In particular, transferred material is carried by the circulation from near the drop surface to along the drop axis.

However if the streamline pattern within the drop is laminar [26], which is often the case [24,25,28,29], the system still relies on diffusive mass transfer to take material from the surface-and-axis towards the internal stagnation point. This problem has been analysed in detail [26], but it was claimed that the systems studied (although formally multi-component ones) actually behaved quite similar to single component ones. It is the wish to observe 'true' multi-component effects including the presence of circulation which has prompted the present work.

This paper is laid out as follows. In the next section (i.e. Section 2), the theory of multi-component mass transfer is introduced. After that a special case of multi-component mass transfer is considered (Section 3), whereby one of the components has no imposed concentration difference: this leads to some simplifications in the formulation, and also some insightful physical interpretations of the resulting multi-component coupling terms. Section 4 briefly describes the numerical methodology used to solve the multi-component mass transfer equations. Numerical results are analysed in Section 5, whilst Section 6 offers conclusions.

2. Multi-component theory of mass transfer

The equation that governs multi-component mass transfer can be written [16,26] as:

$$\frac{\partial \boldsymbol{w}}{\partial t} = -Pe\,\boldsymbol{u}\cdot\nabla\boldsymbol{w} + \boldsymbol{\Delta}\nabla^2\boldsymbol{w}. \tag{1}$$

The various terms in this equation can be defined as follows.

The term $\boldsymbol{w}$ is a vector of solute mass fractions, so that with two solutes present w_1 denotes solute 1 and w_2 denotes solute 2. The terms ∇ and ∇^2 are the gradient and Laplacian operators (made dimensionless with respect to the drop radius R). Meanwhile t denotes time. This has been made dimensionless on a diffusive time scale, $R^2/\langle D\rangle$, where R is the drop radius, and $\langle D\rangle$ is a typical diffusivity scale, comprised of the average of the infinite dilution diffusivities of all the various components in the system.

The term Pe is the Peclet number, which is defined as $RU_{drop}/\langle D\rangle$, where U_{drop} is the drop translation speed relative to the continuous phase. Physically Pe represents the ratio between the diffusive time scale and the streamline circulation time scale. A typical value of Pe is of the order of tens of thousands [26], i.e. diffusion is slow and circulation is rapid, but high Pe simulations are numerically stiff and hence expensive to solve. Moreover, for much of a drop's evolution, any high Pe simulation results asymptote towards a 'master curve' [26]. Thus useful intuition can be gained with less numerical expense for $Pe = 1000$ or even $Pe = 100$.

The field $\boldsymbol{u}$ is the velocity field within and around the drop. It is made dimensionless on the scale U_{drop}. For simplicity (and by contrast with a number of other studies [30–33]) we will assume that the velocity field $\boldsymbol{u}$ is steady over time, and that stresses on the drop surface associated with the velocity field are insufficient to deform it out of spherical. Subject to these assumptions, the field $\boldsymbol{u}$ can be determined by (numerical) solution of the Navier–Stokes equations (see e.g. [28,29]) given the drop Reynolds number Re, and also the ratios between internal and external viscosity, and between internal and external density. It has also been shown that truncated Galerkin expansions [24–26,34,35] give acceptable approximations to the velocity fields. In what follows, we shall employ the same truncated Galerkin velocity field as in [26], which corresponds to $Re = 30$ with equal internal and external viscosities, and equal internal and external densities. A sketch of the resulting streamline pattern is shown in Fig. 1. Notice that the field $\boldsymbol{u}$ is axisymmetric, and hence the mass fraction field $\boldsymbol{w}$ is likewise.

The term $\boldsymbol{\Delta}$ is the multi-component diffusivity matrix [16] (made dimensionless on the scale $\langle D\rangle$). In the case where there are two solutes, it is a 2×2 matrix, with elements Δ_{11}, Δ_{12}, Δ_{21}, Δ_{22}. The off-diagonal elements Δ_{12} and Δ_{21} describe the multi-component couplings between the concentration gradient of one solute and the mass flux of another. The off-diagonal elements can be either positive or negative, depending on the direction in which a gradient of one solute drives a flux of the other. Moreover, if the off-diagonal elements vanish, the two solutes behave as independent single component systems.

The elements of the matrix $\boldsymbol{\Delta}$ can be predicted via the so called Maxwell–Stefan theory [10,16,36–39]. These matrix elements are found to be functions of mass fraction. However it has been shown that during the course of a given liquid–liquid extraction operation, the variation of $\boldsymbol{\Delta}$ is quite weak [40]. Thus $\boldsymbol{\Delta}$ can be assumed to be a constant during the course of any given extraction operation. This has already been anticipated in Eq. (1) as the diffusivity $\boldsymbol{\Delta}$ has been taken outside the Laplacian operator. More details regarding $\boldsymbol{\Delta}$ will be given presently.

Eq. (1) needs to be solved with appropriate sets of initial conditions and boundary conditions. One has a choice of solving either [27] a coupled/'conjugate' problem (both inside and outside the drop, with mass fluxes and chemical potentials matched on the drop surface), or an external problem (i.e. outside the drop only) or an internal problem (i.e. inside the drop only). Technically it is the (more complicated) coupled problem which should be solved, whereas the external and internal problems are merely approximations. The external problem tends to be most relevant for extraction from a gas bubble [15,41] rather than the liquid drop case (on the grounds that mass transport tends to be extremely rapid in the gas phase, implying the transport in the external liquid phase is the rate-limiting step). It has been claimed however [26] that the internal problem may be a reasonable approximation to the full coupled liquid–liquid problem, especially in the limit of large Pe. The reason is as follows. Liquid inside the drop circulates around many times as mass transfer proceeds, whereas (in the frame of reference of the drop) liquid outside the drop flows past the drop surface once

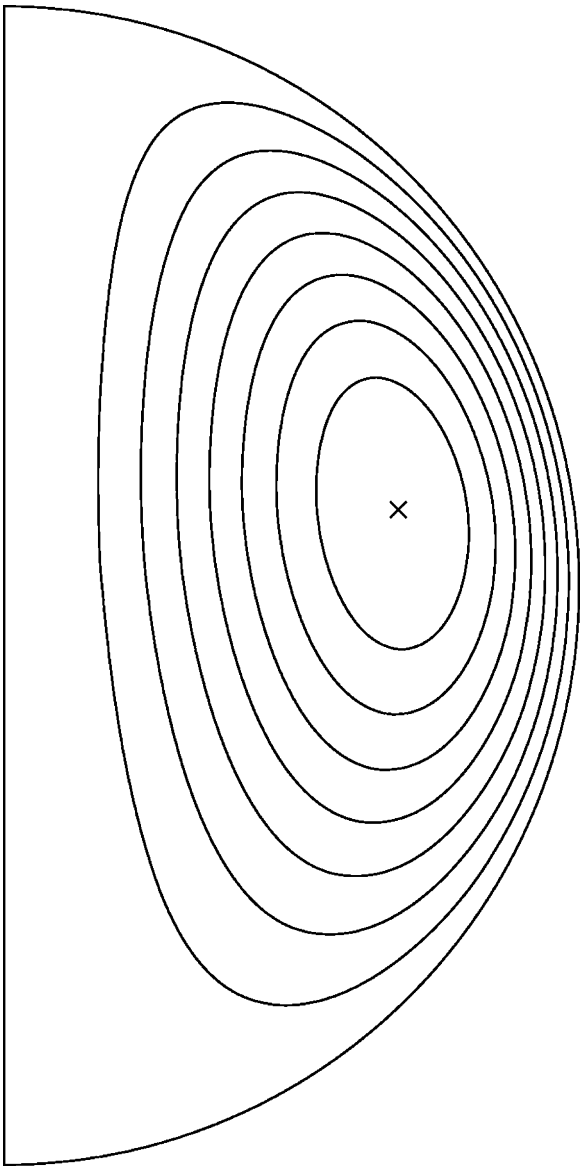

Fig. 1. Streamline pattern determined from a truncated Galerkin expansion for a circulating drop with Reynolds number $Re = 30$. Fluid viscosities are assumed equal inside and outside, as are fluid densities.

only. Fluid elements outside the drop therefore have less time to exchange mass amongst themselves (and so exchange mass over a smaller distance) than those inside the drop. If concentration differences tend to be realised over smaller distances outside the drop than inside it, this means the concentration differences must also be smaller outside to keep the fluxes matched. Hence, in the interests of simplicity, we will solve only internal problems, for which initial uniform solute mass fractions w_1^o and w_2^o are specified, and for which steady boundary mass fractions w_1^R and w_2^R are given.

The internal problem must be solved for all times $t \geq 0$, and (in spherical polar coordinates) dimensionless radial coordinates $0 \leq r \leq 1$ and polar angles $0 \leq \theta \leq \pi$. The azimuthal angle is irrelevant because both $\boldsymbol{u}$ and $\boldsymbol{w}$ are axisymmetric. Initial conditions applicable at $t = 0$ for all dimensionless radial coordinates $0 \leq r < 1$ and polar angles $0 \leq \theta \leq \pi$ are

$$w_1 = w_1^o, \qquad w_2 = w_2^o, \tag{2}$$

where w_1^o and w_2^o are considered uniform over the entire drop. Meanwhile boundary conditions applicable at the drop surface $r = 1$ for all $t > 0$ and $0 \leq \theta \leq \pi$ are

$$w_1 = w_1^R, \qquad w_2 = w_2^R, \tag{3}$$

where w_1^R and w_2^R are considered steady over time and uniform with respect to polar angle.

Specifically we will consider two sets of conditions, one consistent with previous work [26,40]

$$w_1^o = 0.2, \qquad w_1^R = 0.3, \qquad w_2^o = 0.6, \qquad w_2^R = 0.4, \tag{4}$$

and one sharing the same 'mid-range' mass fractions $(w_1^o + w_1^R)/2$ and $(w_2^o + w_2^R)/2$

$$w_1^o = 0.2, \qquad w_1^R = 0.3, \qquad w_2^o = 0.5, \qquad w_2^R = 0.5. \tag{5}$$

For both Eqs. (4) and (5) we say that a concentration difference is imposed for component 1, i.e. $w_1^o \neq w_1^R$. In Eq. (4) there is likewise an imposed concentration difference for component 2, i.e. $w_2^o \neq w_2^R$. In Eq. (5) however $w_2^o = w_2^R$, meaning that no concentration difference is imposed for component 2.

Return now to consider the dimensionless diffusivity matrix $\boldsymbol{\Delta}$. The elements of the matrix $\boldsymbol{\Delta}$ are treated as constant during the course of any given extraction operation, although their values depend on the regime of parameter space in which the operation is taking place. The following values have been computed [26,40] at the 'mid-range' mass fraction and appropriate to the case where component 1 is acetone with $w_1 = 0.25$, component 2 is methanol with $w_2 = 0.5$, and they are both in a benzene solvent[1] with mass fraction $1 - w_1 - w_2 = 0.25$

$$\boldsymbol{\Delta} = \begin{pmatrix} \Delta_{11} & \Delta_{12} \\ \Delta_{21} & \Delta_{22} \end{pmatrix} = \begin{pmatrix} 0.905 & 0.112 \\ -0.041 & 0.362 \end{pmatrix}. \tag{6}$$

It should be noted that – in this particular system – Δ_{11} and Δ_{22} are both significantly larger than Δ_{12} and Δ_{21}. Indeed, if Δ_{12} and Δ_{21} were identically zero, then Eq. (1) would describe two completely independent single component transfers, and clearly with small Δ_{12} and Δ_{21} we are 'close' to that situation.

This then begs the question whether there are any cases for which a system with Δ given by Eq. (1) cannot be approximated by independent single component transfers. As will be demonstrated there is one important case where inherently multi-component effects must be retained, namely one where a concentration difference of component 1 say is imposed, but no concentration difference of component 2 is imposed: see e.g. the boundary and initial conditions of Eq. (5). A single component transfer for component 2 would predict no transfer whatsoever. A multi-component system would predict transfer of component 2 (even though the initial state and, if transfer is allowed to proceed for sufficiently long, the final state would be the same). If we are concerned about component 2 deviating too far from some target purity level during the course of its evolution, solving the multi-component system is essential.

3. Multi-component effects without an imposed concentration difference of a particular component

The usual approach [6–8,26,40] to solving the coupled multi-component equation (1) is to use a matrix transformation to diagonalize $\boldsymbol{\Delta}$, solve for the evolution of decoupled 'pseudo-component' concentrations, and then invert the matrix transformation to recover the 'true' components. We have

[1] It is not necessary that solutes be present in a mass fraction much smaller than the solvent, and indeed for this case they are not. The Maxwell–Stefan tvfheory is sufficiently general that one component can be arbitrarily designated solvent, and all other components solute. Moreover, if that designation is changed, the matrix $\boldsymbol{\Delta}$ transforms in a well-defined way [16].

employed such an approach in our simulations. However in the case where there is no imposed concentration difference of a particular component (component 2 say), it is possible to perform some useful analysis in terms of the 'true' components, without needing to transform to the 'pseudo-component' system.

The basis of this analysis is as follows. If there is no imposed concentration difference of component 2, then we noted above that transfer of component 2 is very dependent on that of component 1. The converse however is not true. Component 1 evolves due to its own imposed concentration difference, largely independently of component 2.

Mathematically this can be explained as follows. In Eq. (1), the effect of component 2 upon component 1 is represented by the term $\Delta_{12}\nabla^2 w_2$. As was stated previously, the coupling coefficient Δ_{12} is relatively small. The gradient of w_2 (and hence $\nabla^2 w_2$) is likewise small, since w_2 is only driven away from its initial value w_2^o (also assumed equal to w_2^R here) by the term $\Delta_{21}\nabla^2 w_1$, again with the coupling coefficient Δ_{21} being relatively small. Component 2 thereby has only a negligible second order effect on component 1.

The equations to be solved therefore are:

$$\frac{\partial w_1}{\partial t} = -Pe\,\boldsymbol{u}\cdot\nabla w_1 + \Delta_{11}\nabla^2 w_1, \tag{7}$$

$$\frac{\partial w_2}{\partial t} = -Pe\,\boldsymbol{u}\cdot\nabla w_2 + \Delta_{21}\nabla^2 w_1 + \Delta_{22}\nabla^2 w_2. \tag{8}$$

These describe a single component evolution of component 1, followed by an evolution of component 2 driven by a source or sink term $\Delta_{21}\nabla^2 w_1$. (In our case, $\Delta_{12} < 0$ and $w_1^R > w_1^o$, and the term in question corresponds to a sink.[2])

Eqs. (7)–(8) still preclude analytic solution on the grounds that $\boldsymbol{u}$ is a complicated spatial flow field. Analytic progress can be made in the limit of a rigid drop $Pe \to 0$. Analytic solutions derived in this limit can give useful intuition even about the $Pe \gg 1$ case, by remembering that radial gradients in the rigid drop $Pe \to 0$ case map to gradients across streamlines [26,27] in the $Pe \gg 1$ case.

Eq. (7) with $Pe \to 0$ is amenable to a Fourier series solution [26,40,42–44]. Additional simplification is possible if one considers the limits of early time, for which gradients are confined to a thin layer near the drop surface. Via Eq. (8), a bound can then be placed on the value that w_2 deviates from its initial value. This turns out to be (for full details see Appendix A)

$$|w_2 - w_2^o| \le \left|\frac{\Delta_{21}}{\Delta_{11}}(w_1^R - w_1^o)\right| \tag{9}$$

in the case when $\Delta_{22} \ll \Delta_{11}$ and

$$|w_2 - w_2^o| \le \left|\frac{\Delta_{21}}{\Delta_{22}}(w_1^R - w_1^o)\right| \tag{10}$$

in the case when $\Delta_{22} \gg \Delta_{11}$. For our system, see Eq. (6), Δ_{22} is considerably smaller than Δ_{11} and Eq. (9) turns out to be a reasonable bound. This bound is physically useful since it allows a chemical engineer to estimate whether or not multi-component effects allow component 2 to remain within a target purity.

It is evident that the right hand sides of both (9) and (10) depend explicitly on the initial/boundary conditions for the 'transferring' component 1, but not explicitly on mass fraction of the 'non-transferring' (or more precisely 'weakly transferring') component 2. At first sight this is curious if one considers the case where component 2 represents a contaminant present in relatively small but equal amounts in both drop and surrounding continuous phases, and the objective is to ensure its concentration in neither one nor the other phase ever rises above a critical limit. Lack of any explicit dependence on w_2 on the right hand sides of (9) and (10) suggests that the amount that the contaminant mass fraction deviates from its initial (and final) mass fraction is independent of that initial/final value: if the contaminant were present only in very tiny trace amounts, it could (temporarily) experience large relative changes in its mass fraction as the system evolves. This however ignores the fact that Δ_{21} and Δ_{11} have implicit dependence on the regime of component mass fractions being considered. In particular as $w_2 \to 0$, it is possible to demonstrate that $\Delta_{21} \to 0$ also, and this is what then limits the deviations predicted by (9) and (10) when the contaminant component 2 is present only in tiny trace amounts. The particular boundary and initial conditions investigated here (Eqs. (4) and (5)) obviously indicate component 2 being present in substantially more than trace amounts, but as was stated above, these have been selected for consistency with previous work [26].

4. Methodology

Eq. (1) has been solved via the same simulation technique as in [26]. The same set of parameter values was also used, i.e. Peclet numbers $Pe = 100$, $Pe = 1000$ and $Pe = 10{,}000$, with the Reynolds number held fixed[3] at $Re = 30$. The substantial difference is that here boundary and initial conditions given by Eq. (5) are explored, instead of merely Eq. (4), so that 'true' multi-component effects could be investigated, not merely systems which behave like two 'almost' independent single components.

Full details of benchmarking and convergence tests of the simulation technique have already been reported [26]. Briefly the equations in dimensionless form were solved with the commercial finite element package Comsol Multiphysics using a mesh with up to 220,800 degrees of freedom, with element edge lengths down to 0.001. Mesh elements tended to be smaller near the drop surface and drop axis (where more resolution is required), and larger near the internal stagnation point (where less resolution is required). Time steps were adaptive with a maximum permitted time step $0.2/Pe$. Mesh refinement and time-step refinement studies were performed, with differences only in the fourth significant figure. Total CPU time of the code for the most expensive simulation runs with $Pe = 10{,}000$ was up to several hours.

As an additional check, the Comsol results were benchmarked against a completely independent in-house finite difference code [26,35]. The finite difference code had lower resolution (128 radial intervals and 64 angular intervals respectively) and a non-adaptive time step of $0.02/Pe$. Differences between the Comsol finite element and in-house finite difference code were only seen in the third significant figure.

5. Results

This simulation results section is organised into five parts. Section 5.1 examines the evolution of the mass fraction of component 1. This evolution is found to be relatively insensitive, at least in

[2] It is worth mentioning also the case of an arbitrary number of solutes, with concentration differences imposed for all but the last solute component. There are then effectively multiple sources or sinks acting on the last solute component. These sources or sinks can either cooperate or compete, depending on the signs of the relevant off-diagonal elements of the diffusivity matrix, and on the signs of the various concentration differences imposed.

[3] The rationale for fixing Reynolds number whilst varying Peclet number – which physically would necessarily correspond to considering an array of different solvent and solute materials – has been explained in [26]. After a few circulations around the drop, mass fraction data are expected to collapse onto a 'master curve' which is independent of the rate at which fluid elements orbit streamlines – i.e. is independent of Pe – but which remains sensitive to streamline layout – which depends on Re. By fixing Re, better collapse onto the 'master curve' is attained.

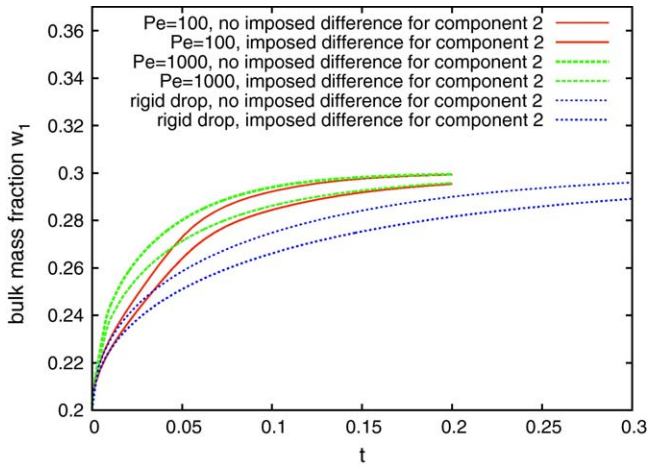

Fig. 2. Bulk w_1 vs time t. Data for the circulating drop (at various Peclet numbers Pe) and for the rigid drop are shown. Some data have an imposed concentration difference for component 2, whilst other data do not.

qualitative terms, to whether or not a concentration difference of component 2 is imposed. This leads to the conclusion that multi-component effects are comparatively weak in this system, and will only become most clearly evident for a component with no imposed concentration difference. The focus in the remaining four parts is then on component 2 with no imposed concentration difference. Section 5.2 deals with bulk (i.e. volume-averaged) concentration values, whilst Sections 5.3–5.5 deal with pointwise concentration data, for the rigid drop in Section 5.3, and for the circulating drop at $Pe = 100$ (Section 5.4) and $Pe = 1000$ (Section 5.5).

5.1. Bulk mass fractions for component 1

Fig. 2 shows bulk mass fractions of component 1 vs dimensionless time t, for a rigid drop and also a circulating drop with $Pe = 100$ and $Pe = 1000$. Results are shown both in the case where there is an imposed concentration difference of component 2 (initial and boundary conditions given by Eq. (4)), and in the case where there is no imposed concentration difference of component 2 (initial and boundary conditions given by Eq. (5)).

In Fig. 2 we see that the circulating drop cases evolve somewhat faster than the rigid drop case. The explanation has been given previously [26]: in the presence of circulation, mass tends to be advected along streamlines [19] and only needs to diffuse from the surface and axis to the internal stagnation point, rather than from the surface to the drop centre. The required diffusion distance is less in the presence of circulation, so the mass transfer is faster.

For our present purposes, it is more important to compare and contrast the effect of using different initial and boundary conditions Eq. (4) vs using Eq. (5). Both for rigid and circulating drops, the presence of an imposed concentration difference of component 2 causes a slight slowing down in the evolution of component 1.

This can be explained as follows. According to Eq. (4), the imposed concentration difference of component 2 causes component 2 to flow out of the drop. Since the matrix element Δ_{12} is positive, this makes a small contribution to component 1 flux out of the drop. This is opposed to the main flux of component 1 which is into the drop and associated with the imposed concentration difference for that component.[4]

The slow-down in the evolution of component 1 (in the presence of an imposed gradient of component 2) can also be expressed in terms of the matrix theory [6–8,26,40] where coupled component concentrations are re-expressed in terms of decoupled 'pseudo-component' concentrations. The system described by Eq. (4) upon decoupling contains a mixture of a 'fast' pseudo-component (rapid approach to equilibrium) and another 'slower' one (slower approach to equilibrium). At long times the final approach to equilibrium is dominated entirely by the 'slow' pseudo-component mode. In the system described by Eq. (5) by contrast, (virtually) none of the 'slow' pseudo-component is excited in the first place, and the 'fast' mode is therefore dominant. Thus quite different timescales to equilibrate the drop are seen depending on whether Eq. (4) or (5) is used.

Nevertheless the overall impact on component 1 of switching between Eqs. (4) and (5) is not massive, especially when the (sometimes considerable [35]) uncertainties in diffusivity values are taken into account. Qualitatively the two behaviours arising from (4) and (5) look the same. In other words, the evolution of the mass fraction of component 1 is only weakly affected by the presence of component 2, and to a reasonable first approximation, component 1 undergoes mass transfer similar to a single component. This then confirms the claim [26] that (even though this is formally a multi-component problem), if significant concentration differences of both component 1 and component 2 are initially imposed, then components 1 and 2 evolve very roughly independently of one another. This follows because the off-diagonal components of the diffusivity matrix Δ_{21} and Δ_{12} are signficantly smaller than the diagonal components Δ_{11} and Δ_{22}. In such a system, the only way to see a 'true' multi-component effect is (in a two solute system) to impose a concentration difference on one component, but not the other: multi-component effects are then observed for the latter component. In all of what follows we impose a concentration difference as per Eq. (5) on component 1 but not on component 2, and we consider the evolution of component 2.

5.2. Bulk mass fractions for component 2

In the case $w_2^o = w_2^R = 0.5$, Fig. 3 shows the evolution of bulk (i.e. volume-averaged) mass fraction w_2 vs time t. Mass fraction initially falls with time t, reaches a minimum and subsequently rises back to the initial value (which is consistent with the claim that the term $\Delta_{21}\nabla^2 w_1$ represents a mass sink). Interestingly the minimum value of bulk w_2 is fairly similar for the rigid drop case and the circulating drop cases: it just occurs at earlier time in the circulating drop case. Thus the rigid drop case shows the slowest evolution, whereas the circulating drop cases (shown for $Pe = 100$, $Pe = 1000$ and $Pe = 10{,}000$) evolve faster. After a certain delay time (associated with the $O(1/Pe)$ time required to execute one streamline orbit around the drop) all the circulating drop data fall onto what might be termed a 'master curve'. Based on the findings of earlier work [26,27], the mass fraction of w_2 is then expected to be uniform along streamlines, but non-uniformities still persist in the cross-stream direction, and diffusion remains active in that direction.

Also shown for completeness on Fig. 3 are predictions with $Pe = 10{,}000$ of a model of Uribe-Ramirez and Korchinsky [24–26]. This model assumes good mixing in the drop interior, rather than mass fraction being tied to streamlines. The (unwarranted) assumption of good mixing causes the Uribe-Ramirez and Korchin-

[4] It is worth noting that the coupling which causes a slight slow-down in the evolution of component 1 relies on having *both* a non-zero off-diagonal matrix element and having a non-zero imposed concentration difference of component 2. Were we to solve using Eq. (4) (i.e. an imposed concentration difference of both components 1 and 2) but suppressing the off-diagonal terms of the $\mathbf{\Delta}$ matrix, we would obtain essentially indistinguishable data as far as component 1 is concerned as using Eq. (5) (i.e. no imposed concentration difference of component 2) but retaining the off-diagonal terms of the $\mathbf{\Delta}$ matrix.

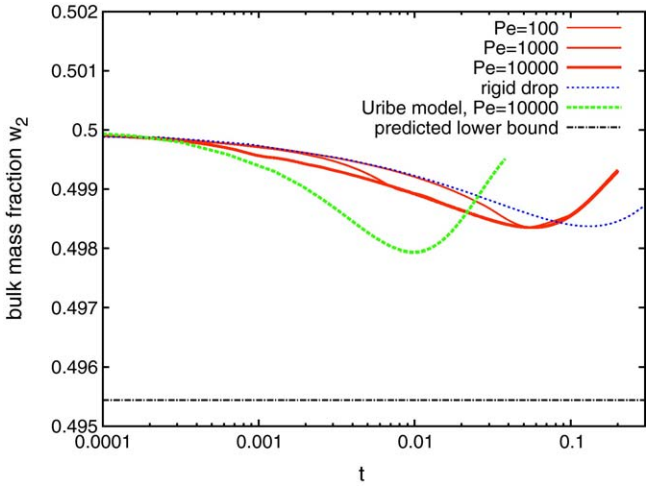

Fig. 3. Bulk w_2 vs time t. Data for the circulating drop (at various Peclet numbers Pe) and for the rigid drop are shown. No concentration difference for component 2 is imposed.

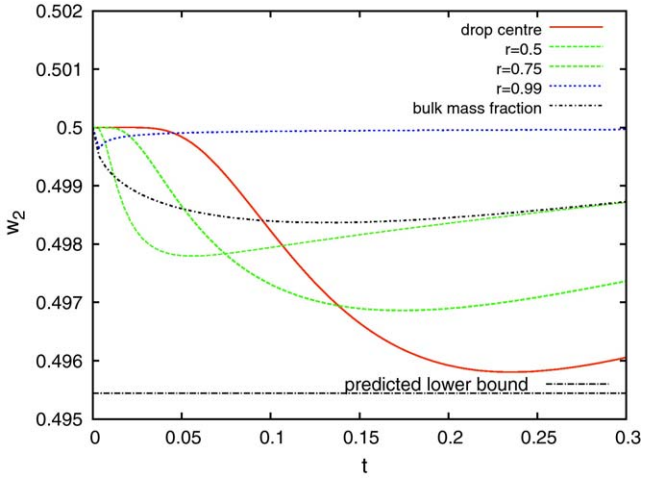

Fig. 4. Time evolution of w_2 at various positions in a rigid drop.

sky model to evolve too quickly, a feature which has already been discussed in the literature [26].

Fig. 3 also indicates a lower bound on the value of w_2. This is given in Eq. (9) and is derived in Appendix A. None of the bulk w_2 data shown approach remarkably closely to the lower bound. This is not surprising. The lower bound as derived in Appendix A applies pointwise at any given position in the drop. However not all positions in the drop approach the bound at the same time. The bulk mass fraction which is an average over various positions at a given time is not expected to approach too closely to the bound.

Based on the lower bound an engineer could predict confidently in this system that mass fraction of component 2 – initially equal to 0.5 – could not fall below 0.495. If the purity specification is stricter than that (e.g. if component 2 is required to have a mass fraction at least 0.499) then the engineer would need to design the liquid–liquid extraction system such that the drop residence time is, according to Fig. 3, at least 0.2 dimensionless units (for a circulating drop[5]) and even longer than that for a rigid drop.

5.3. Rigid drop pointwise data

To date we have only considered bulk (i.e. volume-averaged) mass fraction data. It is instructive however to examine data points at individual positions in the drop to see their evolution over time (and also to see how closely they approach to the aforementioned lower bound). In the first instance rigid drop data are examined: see Fig. 4.

Data points nearest the surface are found to depart from w_2^o sooner than points further from the surface, but also begin to return to w_2^o earlier, which is in line with predictions in Appendix A. Overall it is seen that points nearer the surface deviate less from w_2^o than points further from away from it. This is interesting because the (somewhat simplified) predictions in Appendix A imply that the maximum deviation over time is independent of point position. Some possible explanations of this discrepancy are as follows.

The position-independent bound on how much w_2 deviates, indicated on Fig. 4, has been derived assuming that $\Delta_{22} \ll \Delta_{11}$, whereas in reality the ratio Δ_{22}/Δ_{11} is only about 0.4: this may be a source of discrepancy. If $|Z|$ denotes the dimensionless distance between an arbitrary point and the drop surface, approach to the bound is only theoretically applicable (see Appendix A) for times $Z^2/\Delta_{11} \ll t \ll Z^2/\Delta_{22}$, which corresponds to a very small time interval as $|Z|$ decreases. Physically this can be understood as follows. The role of a small but finite Δ_{22} (as opposed to infinitesimal Δ_{22} whereby $\Delta_{22} \ll \Delta_{11}$) must be to smear out the effect of the mass sink – presumably over a distance $\sqrt{\Delta_{22}t}$. If the distance $|Z|$ to the drop surface is less than $\sqrt{\Delta_{22}t}$, then the smearing zone incorporates the drop surface, and the point Z is aware of and dominated by the boundary condition $w_2 = w_2^R \equiv w_2^o$ imposed on the surface, rather than deviating to the extent that Eq. (9) permits. If $|Z|$ is small, this dominance by the surface boundary condition is felt at very early times.

There is also the fact that the analysis of Appendix A assumes a Cartesian rather than a spherical geometry. The effects of spherical geometry can be qualitatively explained as follows. The drop is a unit sphere in dimensionless coordinates. Consider a subdomain within the unit sphere between the centre and an arbitrary radial location r. The mass transfer rate into the subdomain is the product of the incoming flux $\boldsymbol{\Delta}\partial\boldsymbol{w}/\partial r$ and the surface area $4\pi r^2$. This mass transfer rate can be equated to the product of the subdomain volume $(4/3)\pi r^3$ and the rate of change of average mass fraction within the subdomain (denoted $\partial\langle\boldsymbol{w}\rangle/\partial t$ say). The smaller the subdomain (i.e. the smaller the r value chosen) the larger the surface to volume ratio and the more susceptible the average mass fraction becomes to a given incoming flux. Indeed the point at the centre of the drop very nearly achieves the lower bound equation (9) whereas the bulk w_2 does not. This reflects the small contribution that the neighbourhood of the drop centre makes to the bulk w_2.

There is yet another possible physical effect which is excluded from the current model, but which may cause (bulk) w_2 to approach closer to the lower bound. This is the change in drop volume induced by the flux of component 1. In the present case, component 1 is entering the drop (Fig. 2) so the drop volume should grow. This will lead to a reduction of mass fraction w_2 additional to what has been calculated here. The effect is temporary as eventually the drop must equilibrate with the surrounding medium in spite of its volume change.

5.4. Pe = 100 pointwise data

Fig. 5 is similar to Fig. 4 except for a circulating drop with $Pe = 100$ instead of for a rigid drop. Again the fastest response is seen near

[5] Using the data for drop radius R and diffusivity $\langle D\rangle$ quoted in [26], this corresponds to about 60 s of dimensional time, longer than the 10 s residence time that is currently typical in liquid–liquid extractors [26]. A reduction in drop radius by a factor of three will however ensure that the specified purity is achieved well within 10 s.

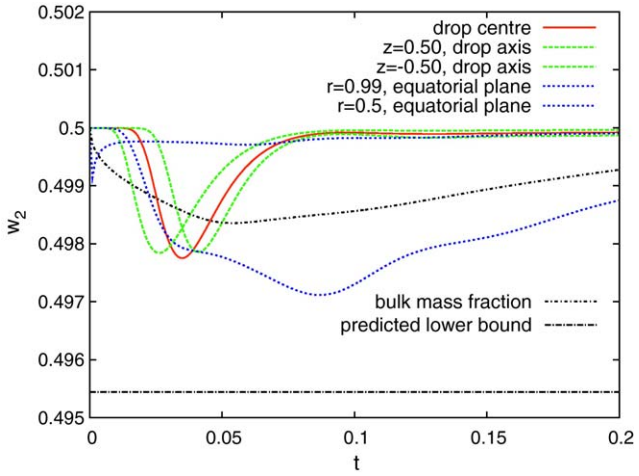

Fig. 5. Time evolution of w_2 at various positions in a circulating drop with $Pe = 100$.

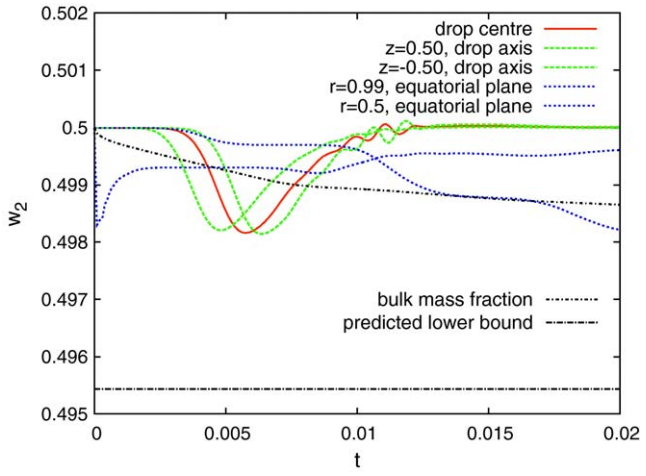

Fig. 6. Time evolution of w_2 at various positions in a circulating drop with $Pe = 1000$.

the surface (see e.g. the point with radial coordinate $r_2 = 0.99$ on the equatorial plane). However, analogously to [26], a fast response is also now seen on the drop axis, owing to advection of material from near the surface along the axis. Specifically three axis points are shown: the drop centre, and a point with axial coordinate $z = 0.5$ (above the centre), and one with axial coordinate $z = -0.5$ (below the centre). Although all three axis points evolve relatively quickly, the point above (below) the centre evolves slightly slower (faster) than the centre point itself, as the different travel times for fluid elements that start near the surface and advect material to those axis points must be taken into account [26].

Out of all the various points considered, the slowest evolution is seen for the point $r = 0.5$ on the equatorial plane. This is unsurprising, given that this point is not too far from the internal stagnation point (with $r \sim 0.7$) and diffusion proceeds from streamline to streamline [26] in the circulating drop case.

The equatorial data for $r = 0.5$ also show a larger deviation from w_2^o than any of the other points considered. As for the rigid drop case, this may just be associated with a longer time period between when w_2 starts to decrease significantly and when it starts to return back to its initial value again. Alternatively, again as in the rigid drop discussion, it may be a geometric effect: there is a lot more drop volume enclosed by streamlines that pass near the drop surface and/or axis, than enclosed by streamlines that pass the neighbourhood of the internal stagnation point.

Note that there are some oscillations superposed on the data for $r = 0.5$ on the equatorial plane. These are not a numerical artifact, but rather are associated with the fact that different streamlines have different orbit periods, and so advect mass along at different rates. For the first few orbit periods before uniformity of mass fraction along streamlines is achieved, this produces a complicated concentration field with oscillations superposed [26,27].

5.5. *Pe = 1000 pointwise data*

Fig. 6 shows data for $Pe = 1000$. Note the different scale on the graph: compared to Fig. 5 circulations are 10 times faster, and the scale plotted is 10 times shorter.

The data make it clear that concentrations on the axis evolve on the circulation time scale. Note that weak high frequency oscillations are seen in the on-axis data. These appear to be an artifact of the numerical scheme as they have a period of just a few time steps. There was no smoothing via e.g. upwinding [45,46] implemented in the numerical scheme and the Galerkin expansion expression employed here for the flow-field (following [24–26,34]) actually has a mild singularity in the neighbourhood of the drop centre.[6] These numerical oscillations should not be confused with e.g. physical oscillations on the time scale of one drop circulation which are seen e.g. for the evolution at the point $r = 0.5$ on the equatorial plane. As has already been discussed, such oscillations are associated with different streamlines having different orbit times. Moreover in order to see the complete evolution of the point $r = 0.5$ on the equatorial plane, it is necessary to look on a diffusive (not an advective) time scale. This can be seen in Fig. 7 still for the case $Pe = 1000$. Oscillations are suppressed after several streamline orbits, and the equatorial plane data at $r = 0.5$ return to the value w_2^o on a time scale remarkably similar to what is observed when $Pe = 100$ (Fig. 5).

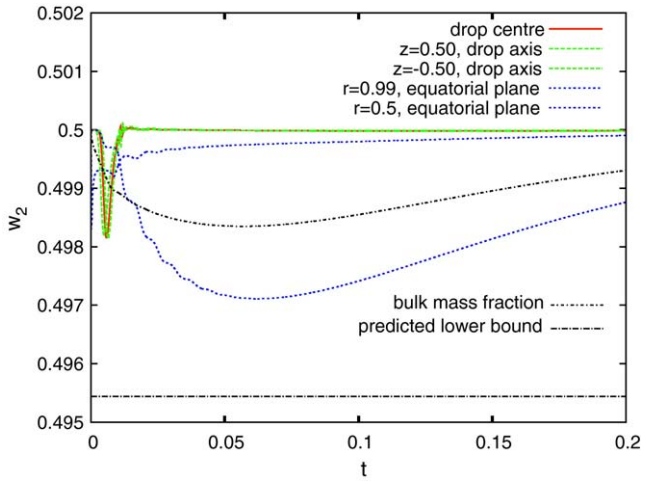

Fig. 7. Longer time scale evolution of w_2 at various positions in a circulating drop with $Pe = 1000$.

It is possible to examine analogous data to Figs. 5–7 for the case $Pe = 10{,}000$. Qualitatively the findings are similar, but an even bigger disparity is observed between the the advective time scale (short; applicable to the evolution of mass fraction for points on streamlines passing near the surface and along the axis) and the diffusive

[6] Specifically the velocity differs slightly in the limit as radial coordinate $r \to 0$ depending on the polar angle θ. It is curious that this singularity has never been noted previously in the literature, but some past analyses using this particular flow-field – e.g. that of [24,25] – focused exclusively on mass transfer in the neighbourhood of the drop surface $r = 1$ where the flow-field singularity is irrelevant.

time scale (long; applicable to the evolution of mass fraction for locations near the internal stagnation point).

6. Conclusions

Numerical simulation results for multi-component mass transfer in drops have been considered. Specifically a system with two solute components in a solvent has been studied. The theory of multi-component mass transfer implies that the mass fluxes and concentration gradients should be coupled between one solute and the other. The strength of this coupling is measured by off-diagonal terms in a diffusivity matrix. Coupling will be strong when these off-diagonal matrix elements are comparable with the diagonal ones. However in the particular case studied here (corresponding to the system acetone–methanol–benzene), the off-diagonal terms are actually quite weak. In that case, naively it might be thought that, to a reasonable approximation, multi-component effects might be dispensed with altogether. However this is found not to be always the case. Whether or not multi-component effects need to be retained depends on the set of initial and boundary conditions imposed on the component mass fractions.

In order to illustrate this point, two sets of initial and boundary conditions have been considered, one where a concentration difference between the (initial) interior of the drop and the drop surface is imposed for both components, and the other where a concentration difference is imposed for one component but not the other. Since (as was pointed out above) off-diagonal elements in the diffusivity matrix are relatively weak compared to diagonal ones, the case where both components have imposed concentration differences can be understood at least very approximately/qualitatively as two independent single component mass transfer processes.

True multi-component effects are nevertheless seen if a concentration difference is imposed for one component but not the other. Mass transfer occurs even for the component with no imposed concentration difference, whereas none whatsoever would take place for an independent single component process. The component with an imposed concentration difference is virtually uninfluenced by the presence of the one with no imposed difference. The role of the former component is then to provide a mass source or sink for the latter.

Knowledge about the strength of this source or sink is important. If left to transfer mass for an arbitrarily long time, the component with no imposed concentration difference has the same final concentration as its initial one. The strength of the source or sink provides an upper bound on the amount that the concentration can deviate from this initial/final concentration during the course of its evolution. This bound can then be used to check whether or not component concentration is likely to deviate outside some specified target purity. For consistency with previous work [26], we have considered a case where the 'non-transferring' or 'weakly transferring' component is present in substantial amounts. However the bound on purity may be particularly important/relevant when this component is a contaminant present in just small trace amounts. Estimating the bound on purity only requires knowledge of initial and boundary conditions for the mass fractions of various solutes, as well as predictions of the elements of a diffusivity matrix in the mass fraction parameter range of interest (which are available via the Maxwell–Stefan theory [16]).

Results have been presented both for a rigid drop and for a circulating drop. The maximum amount that the volume-averaged component concentration deviates from its initial/final value is insensitive to whether the drop is rigid or circulating. However the rate of deviation and return is slower for a rigid drop than a circulating one (which will be relevant to designing a liquid-liquid extraction system if it is necessary to wait for the component concentration to return to within some specified target purity). Moreover the order in time at which concentration at different locations within the drop evolves is sensitive to the presence or absence of circulation. Deviations are seen earliest near the surface for the rigid drop, and latest near the centre. Meanwhile deviations are seen earliest near the surface and axis for the circulating drop, and latest near the internal stagnation point. In both the rigid and circulating drop cases, points which show earlier deviation away from the initial/final value also show a more rapid return back to that initial/final value.

Acknowledgements

Paul Grassia acknowledges support from UMR8085 LPTM and CNRS via contract 240335.

Appendix A.

We consider the case of multi-component mass transfer in a rigid drop in the limit of early times (when the geometry can be approximated as Cartesian) with two solutes and with no concentration difference imposed on solute component 2. Solute component 1 then evolves independently of component 2 according to

$$\frac{\partial w_1}{\partial t} = \Delta_{11}\frac{\partial^2 w_1}{\partial Z^2}. \tag{A.1}$$

Here we have defined a (dimensionless) distance coordinate Z in terms of the dimensionless radial coordinate r via $Z = r - 1$. Since we focus on internal problems, we are interested in the domain $Z < 0$. The solution for w_1 is

$$w_1 = w_1^o + (w_1^R - w_1^o)\left(1 + \mathrm{erf}\frac{Z}{2\sqrt{\Delta_{11}t}}\right), \tag{A.2}$$

where w_1^o is the initial value and w_1^R is the boundary value.

The equation governing the evolution of w_2 is

$$\frac{\partial w_2}{\partial t} = \Delta_{22}\frac{\partial^2 w_2}{\partial Z^2} + \Delta_{21}\frac{\partial^2 w_1}{\partial Z^2}. \tag{A.3}$$

Physically this states that the rate of change of w_2 depends on diffusion of w_2 and also a mass source or sink term $\Delta_{21}\partial^2 w_1/\partial Z^2$. Since $\Delta_{21} < 0$ in Eq. (6) and since $w_1^R > w_1^o$ in Eq. (5), we are dealing with a mass sink. The initial value for w_2 is w_2^o (and this is also the boundary value).

Rather than giving a general solution to Eq. (A.3), we consider two extreme limits either $\Delta_{22} \ll \Delta_{11}$ or $\Delta_{11} \ll \Delta_{22}$. Remember throughout that since Δ_{11} and Δ_{22} are quantities that have been made dimensionless based on $\langle D \rangle$ (the average infinite dilution diffusivity over the entire system), the larger value out of Δ_{11} or Δ_{22} must be a quantity of order unity. The actual values of Δ_{11} and Δ_{22} are reported in Eq. (6) for the system acetone–methanol–benzene. Clearly this particular system (as considered here, with an imposed concentration difference for acetone, but no imposed difference for methanol) is closer to the limit $\Delta_{22} \ll \Delta_{11}$. However were we to consider an alternative case (with a concentration difference imposed for methanol, but not acetone), then (after suitable relabelling of subscripts) we would be closer to a system with $\Delta_{22} \ll \Delta_{11}$. Thus both extremes are considered here for completeness.

A.1. Limiting case: $\Delta_{22} \ll \Delta_{11}$

As a first approximation the term $\Delta_{22}\partial^2 w_2/\partial Z^2$ in Eq. (A.3) can be dropped, and a so called 'outer' solution can be obtained

$$w_2 - w_2^o = \frac{\Delta_{21}}{\Delta_{11}}(w_1 - w_1^o). \tag{A.4}$$

Thus changes in w_2 are directly proportional to changes in w_1. At any given time, points which have $|Z| = O(\sqrt{\Delta_{11}t})$ will have seen significant changes in w_1 and hence in w_2. In principle w_2 can deviate from w_2^o by a magnitude of up to $|\Delta_{21}(w_1^R - w_1^o)/\Delta_{11}|$ (hence the bound reported in Eq. (9)). Points which have $|Z| \gg O(\sqrt{\Delta_{11}t})$ will have not yet seen a change in w_1 and hence will have not yet seen a change in w_2. At a distance $|Z|$ from the drop surface, the time scale on which w_2 starts to change is $O(Z^2/\Delta_{11})$.

Eq. (A.4) cannot be a full solution for w_2 as it fails to satisfy a boundary condition that $w_2 = w_2^o$ in the limit $Z \to 0$. The solution (A.4) must be therefore be matched [47] onto an inner solution which applies for $|Z| \le O(\sqrt{\Delta_{22}t})$.

Remarkably the inner solution can be obtained by solving simply

$$\frac{\partial w_2}{\partial t} = \Delta_{22}\frac{\partial^2 w_2}{\partial Z^2}, \tag{A.5}$$

i.e. the mass sink term plays no role. This is because the sink term vanishes both when $|Z| \gg O(\sqrt{\Delta_{11}t})$ and when $|Z| \ll O(\sqrt{\Delta_{11}t})$ so it certainly vanishes when $|Z| = O(\sqrt{\Delta_{22}t}) \ll O(\sqrt{\Delta_{11}t})$. The solution is

$$w_2 = w_2^o - (w_1^R - w_1^o)\frac{\Delta_{21}}{\Delta_{11}}\,\mathrm{erf}\frac{Z}{2\sqrt{\Delta_{22}t}}. \tag{A.6}$$

It is easy to check that the $Z \to -\infty$ limit of the inner solution matches the $Z \to 0$ limit of the outer solution. Based on the inner solution, it is seen that the time scale on which a point at distance $|Z|$ from the drop surface begins to return to $w_2 \approx w_2^o$ is $O(Z^2/\Delta_{22})$. Thus points further from the drop surface both deviate from $w_2 \approx w_2^o$ later and also return to $w_2 \approx w_2^o$ later.

A.2. Limiting case: $\Delta_{11} \ll \Delta_{22}$

The mass sink is still confined to a region $|Z| = O(\sqrt{\Delta_{11}t})$ but the diffusive terms $\Delta_{22}\partial^2 w_2/\partial Z^2$ can now influence component 2 concentration far beyond the extent of the sink, out to distances $|Z| = O(\sqrt{\Delta_{22}t}) \gg O(\sqrt{\Delta_{11}t})$.

As far as this 'far field' $|Z| = O(\sqrt{\Delta_{22}t})$ solution is concerned, it does not matter whether the mass is removed over a distributed sink of extent $O(\sqrt{\Delta_{11}t})$ or alternatively by imposing an equivalent flux boundary condition at some arbitrary point $Z = Z_{sink}$ (with $Z_{sink} < 0$ but $|Z_{sink}| = O(\sqrt{\Delta_{11}t}) \ll O(\sqrt{\Delta_{22}t})$). The resulting solution is

$$w_2 = w_2^o + \left(\frac{\Delta_{21}(w_1^R - w_1^o)}{\sqrt{\Delta_{11}\Delta_{22}}}\right)\left(1 + \mathrm{erf}\frac{Z - Z_{sink}}{2\sqrt{\Delta_{22}t}}\right). \tag{A.7}$$

It is relatively easy to demonstrate for this solution that the diffusive flux of w_2 at the point $Z = Z_{sink}$ matches the rate of consumption of mass integrated over the sink.

The problem with this solution is that it does not satisfy the boundary condition that $w_2 = w_2^o$ at $Z = 0$. This can be achieved by adding an equal strength image source term outside the drop at $Z = Z_{source}$ with $Z_{source} > 0$ and in fact $Z_{source} = -Z_{sink}$. The net far field solution is then

$$w_2 = w_2^o + \frac{Z_{source}}{\sqrt{\Delta_{11}t}}\frac{\Delta_{21}(w_1^R - w_1^o)}{\Delta_{22}}\frac{2}{\sqrt{\pi}}\exp - \frac{Z^2}{4\Delta_{22}t}. \tag{A.8}$$

Observe that, since $\Delta_{11} \ll \Delta_{22}$ here, w_2 predicted by Eq. (A.8) (sink plus image source) is smaller in magnitude than Eq. (A.7) (sink only). Physically this means that almost all of the effect of the mass sink is compensated for by w_2 diffusing into the drop at the $Z = 0$ boundary, with only a weak effect surviving into the far field.

Under these circumstances it is then possible to derive a 'near field' solution (applicable for the region $|Z| = O(\sqrt{\Delta_{11}t}) \ll O(\sqrt{\Delta_{22}t})$) with a (quasi)steady flux balance between diffusive and sink terms. The result is

$$w_2 = w_2^o - \frac{\Delta_{21}}{\Delta_{22}}(w_1 - w_1^R). \tag{A.9}$$

By matching the $Z \to 0$ limit of the far field solution to the $Z \to -\infty$ limit of the near field solution, it is possible to deduce that $Z_{source}/\sqrt{\Delta_{11}t} = \sqrt{\pi}/2$. For a given Z, deviation from $w_2 \approx w_2^o$ starts when t becomes $O(Z^2/\Delta_{22})$ (deduced via the far field solution) and ceases when t exceeds $O(Z^2/\Delta_{11})$ (deduced via the near field solution). The magnitude of the deviation is bounded by $|\Delta_{21}(w_1^R - w_1^o)/\Delta_{22}|$, which is the bound reported in Eq. (10).

References

[1] R.E. van Vliet, T.P. Tiemersma, G.J. Krooshof, P.D. Iedema, The use of liquid–liquid extraction in the EPDM solution polymerization process, Industrial and Engineering Chemistry Research 40 (2001) 4586–4595.
[2] L. Li, F. Liu, X.X. Kong, S. Su, Li.F K.A., Investigation of a liquid–liquid extraction system based on non-ionic surfactant–salt–H_2O and mechanism of drug extraction, Analytica Chimica Acta 452 (2002) 321–328.
[3] C.K. Chambliss, T.J. Haverlock, P.V. Bonnesen, N.L. Engle, B.A. Moyer, Selective separation of hydroxide from alkaline nuclear tank waste by liquid–liquid extraction with weak hydroxy acids, Environmental Science and Technology 36 (2002) 1861–1867.
[4] L. Alonso, A. Arce, M. Francisco, O. Rodriguez, A. Soto, Gasoline desulfurization using extraction with [C_8mim][BF_4] ionic liquid, AIChE Journal 53 (2007) 3108–3115.
[5] A. Deep, P.F.M. Correia, J.M.R. de Carvalho, Liquid–liquid extraction and separation of a macro concentration of Fe^{3+}, Industrial and Engineering Chemistry Research 46 (2007) 5707–5714.
[6] H.L. Toor, Solution of the linearised equations of multicomponent mass transfer, AIChE Journal 10 (1964) 448–455.
[7] H.L. Toor, Solution of the linearised equations of multicomponent mass transfer. II. Matrix methods, AIChE Journal 10 (1964) 460–465.
[8] W.E. Stewart, R. Prober, Matrix calculation of multicomponent mass transfer in isothermal systems, Industrial and Engineering Chemistry Fundamentals 3 (1964) 224–235.
[9] H.T. Cullinan, A critique of some approximate theories of multicomponent diffusion in liquid systems, Computers and Chemical Engineering 4 (1972) 248–252.
[10] R. Krishna, G.L. Standart, A multicomponent film model incorporating a general matrix method of solution to the Maxwell–Stefan equations, AIChE Journal 22 (1976) 383–389.
[11] R. Krishna, G.L. Standart, Mass and energy transfer in multicomponent systems, Chemical Engineering Communications 3 (1979) 201–275.
[12] J. Bandrowski, A. Kubaczka, On the prediction of diffusivities in multicomponent liquid systems, Chemical Engineering Science 37 (1982) 1309–1313.
[13] A. Kubaczka, J. Bandrowski, Solutions of a system of multicomponent mass transport equations for mixtures of real fluids, Chemical Engineering Science 46 (1991) 539–556.
[14] M.J. Brodkorb, D. Bosse, C. von Reden, A. Gorak, M.J. Slater, Single drop mass transfer in ternary and quaternary liquid–liquid extraction systems, Chemical Engineering and Processing 42 (2003) 825–840.
[15] G. Juncu, Unsteady ternary mass transfer from a sphere in creeping flow, International Journal of Thermal Science 44 (2005) 255–266.
[16] R. Taylor, R. Krishna, Multicomponent Mass Transfer, John Wiley and Sons, New York, USA, 1993.
[17] R.B. Bird, W.E. Stewart, E.N. Lightfoot, Transport Phenomena, 1st edition, John Wiley and Sons, New York, 1960.
[18] H. Klocker, H.J. Bart, R. Marr, H. Muller, Mass transfer based on chemical potential theory: $ZnSO_4/H_2SO_4$/D2EHPA, AIChE Journal 43 (1997) 2479–2487.
[19] R. Kronig, J.C. Brink, The theory of extraction from falling droplets, Applied Science Research A2 (1950) 142–154.
[20] E. Ruckenstein, Mass transfer between a single drop and a continuous phase, International Journal of Heat and Mass Transfer 10 (1967) 1785–1792.
[21] B.T. Chao, Transient heat and mass transfer to a translating droplet, Journal of Heat Transfer, Transactions of ASME 91 (1969) 273–280.
[22] W.H. Piarah, A. Paschedag, M. Kraume, Numerical simulation of mass transfer between a single drop and an ambient flow, AIChE Journal 47 (7) (2001) 1701–1704.

[23] M.A. Waheed, M. Henschke, A. Pfennig, Mass transfer by free and forced convection from single spherical liquid drops, International Journal of Heat and Mass Transfer 45 (2002) 4507–4514.
[24] A.R. Uribe-Ramirez, W.J. Korchinsky, Fundamental theory for prediction of single-component mass transfer in liquid drops at intermediate Reynolds numbers ($10 < Re < 250$), Chemical Engineering Science 55 (2000) 3305–3318.
[25] A.R. Uribe-Ramirez, W.J. Korchinsky, Fundamental theory for prediction of multicomponent mass transfer in single-liquid drops at intermediate Reynolds numbers ($10 < Re < 250$), Chemical Engineering Science 55 (2000) 3319–3328.
[26] S. Ubal, C.H. Harrison, P. Grassia, W.J. Korchinsky, Numerical simulation of mass transfer in circulating drops, Chemical Engineering Science 65 (2010) 2934–2956.
[27] G. Juncu, A numerical study of the unsteady heat/mass transfer inside a circulating sphere, International Journal of Heat and Mass Transfer 53 (2010) 3006–3012.
[28] G. Juncu, A numerical study of steady viscous flow past a fluid sphere, International Journal of Heat and Fluid Flow 20 (1999) 414–421.
[29] Y. Yan, H. Lai, C.R. Gentle, J.M. Smith, Numerical analysis of fluid flows inside and around a liquid drop using an incorporation of multi-block iteration and moving mesh, Chemical Engineering Research and Design 80 (2002) 325–331.
[30] P.M. Rose, R.C. Kintner, Mass transfer from large oscillating drops, AIChE Journal 12 (1966) 530–534.
[31] D.S. Dandy, L.G. Leal, Buoyancy-driven motion of a deformable drop through a quiescent liquid at intermediate Reynolds numbers, Journal of Fluid Mechanics 208 (1989) 161–192.
[32] T.W. Li, Z.S. Mao, J.Y. Chen., Experimental and numerical investigations of single drop mass transfer in solvent extraction systems with resistance in both phases, Chinese Journal of Chemical Engineering 10 (2002) 1–14.
[33] C. Yang, Z.S. Mao., Numerical simulation of interphase mass transfer with the level set approach, Chemical Engineering Science 60 (2005) 2643–2660.
[34] Y. Nakano, C. Tien., Approximate solutions of viscous incompressible flow around fluid spheres at intermediate Reynolds numbers, Canadian Journal of Chemical Engineering 52 (1967) 135–140.
[35] C.H. Harrison, Multicomponent mass transfer in liquid–liquid extraction, PhD Thesis, School of Chemical Engineering and Analytical Science, University of Manchester, Manchester, UK, 2006.
[36] R. Krishna, J.A. Wesselingh, The Maxwell–Stefan approach to mass transfer, Chemical Engineering Science 52 (6) (1997) 861–911.
[37] A. Zimmerman, X. Joulia, C. Gourdon, A. Gorak, Maxwell–Stefan approach in extractor design, The Chemical Engineering Journal and the Biochemical Engineering Journal 57 (1995) 229–236.
[38] J. Toutain, J.M. Le Lann, C. Gourdon, X. Joulia, Maxwell–Stefan approach coupled drop population model for the dynamic simulation of liquid–liquid extraction pulsed column, Computers and Chemical Engineering 22 (1998) S379–S386.
[39] K. Tseronis, I.K. Kookos, C. Theodoropoulos, Modelling mass transport in solid oxide fuel cell anodes: a case for a multidimensional dusty gas-based model, Chemical Engineering Science 63 (2008) 5626–5638.
[40] W.J. Korchinsky, P. Grassia, C.H. Harrison, Multicomponent mass transfer in films and rigid drops: the influence of concentration-variable diffusivity, Chemical Engineering Science 64 (2009) 433–442.
[41] G. Juncu, Unsteady heat and/or mass transfer from a fluid sphere in creeping flow, International Journal of Heat and Mass Transfer 44 (2001) 2239–2246.
[42] A.B. Newman, The drying of porous solids: diffusion and surface emission equations, Transactions of AIChE 27 (1931) 203–221.
[43] E.D. Negri, W.J. Korchinsky, Multicomponent mass transfer in spherical rigid drops, Chemical Engineering Science 41 (1986) 2395–2400.
[44] E.D. Negri, C.H. Young, W.J. Korchinsky, High flux, single solute mass transfer in spherical rigid drops, Chemical Engineering Science 41 (1986) 2401–2406.
[45] J.C. Heinrich, P.S. Huyakorn, O.C. Zienkiewicz, A.R. Mitchell, An 'upwind' finite element scheme for two-dimensional convective transport equation, International Journal for Numerical Methods in Engineering 11 (1) (1977) 131–143.
[46] W.H. Press, S.A. Teukolsky, W.T. Vetterling, B.P. Flannery, Numerical Recipes in C. The Art of Scientific Computing, 2nd edition, Cambridge University Press, Cambridge, 1992.
[47] A.H. Nayfeh, Perturbation Methods, Wiley-Interscience, New York, Chichester, 1973.